Geophysical Research Letters

RESEARCH LETTER
10.1029/2021GL096073

Key Points:

- New particle formation is more prevalent off the U.S. East Coast in winter rather than summer
- Ratio of particle number above 3 versus 10 nm peaks above cloud top regardless of season
- Cold and dry conditions during cold air outbreaks coincide with new particle formation

Supporting Information:

Supporting Information may be found in the online version of this article.

Correspondence to:

A. F. Corral,
afcorral@arizona.edu

Citation:

Corral, A. F., Choi, Y., Crosbie, E., Dadashazar, H., DiGangi, J. P., Diskin, G. S., et al. (2022). Cold air outbreaks promote new particle formation off the U.S. East Coast. *Geophysical Research Letters*, *49*, e2021GL096073. https://doi.org/10.1029/2021GL096073

Received 23 SEP 2021
Accepted 22 FEB 2022

Author Contributions:

Conceptualization: Andrea F. Corral, Armin Sorooshian
Formal analysis: Andrea F. Corral, Armin Sorooshian
Funding acquisition: Armin Sorooshian
Methodology: Andrea F. Corral, Armin Sorooshian
Project Administration: Armin Sorooshian
Supervision: Armin Sorooshian
Writing – original draft: Andrea F. Corral, Armin Sorooshian
Writing – review & editing: Andrea F. Corral, Yonghoon Choi, Ewan Crosbie, Hossein Dadashazar, Joshua P. DiGangi, Marta Fenn, David B. Harper, Simon Kirschler, Hongyu Liu, Richard H. Moore, John B. Nowak, Amy Jo Scarino, Shane Seaman, Taylor Shingler, Michael A. Shook, Kenneth L. Thornhill, Christiane Voigt, Bo Zhang, Luke D. Ziemba, Armin Sorooshian

Cold Air Outbreaks Promote New Particle Formation Off the U.S. East Coast

Andrea F. Corral[1], Yonghoon Choi[2,3], Ewan Crosbie[2,3], Hossein Dadashazar[1], Joshua P. DiGangi[2], Glenn S. Diskin[2], Marta Fenn[2,3], David B. Harper[2], Simon Kirschler[4,5], Hongyu Liu[6], Richard H. Moore[2], John B. Nowak[2], Amy Jo Scarino[2,3], Shane Seaman[2], Taylor Shingler[2], Michael A. Shook[2], Kenneth L. Thornhill[2,3], Christiane Voigt[4], Bo Zhang[6], Luke D. Ziemba[2], and Armin Sorooshian[1,7]

[1]Department of Chemical and Environmental Engineering, University of Arizona, Tucson, AZ, USA, [2]NASA Langley Research Center, Hampton, VA, USA, [3]Science Systems and Applications, Inc., Hampton, VA, USA, [4]German Aerospace Center, Institute for Atmospheric Physics, DLR, Oberpfaffenhofen, Germany, [5]Institute of Atmospheric Physics, Johannes Gutenberg-University Mainz, Mainz, Germany, [6]National Institute of Aerospace, Hampton, VA, USA, [7]Department of Hydrology and Atmospheric Sciences, University of Arizona, Tucson, AZ, USA

Abstract New particle formation (NPF) is the dominant contributor to total particle number concentration and plays an important role in the cloud condensation nuclei budget. Airborne data from Aerosol Cloud meTeorology Interactions oVer the western ATlantic Experiment (ACTIVATE) are used to address seasonal NPF statistics and factors related to NPF in and around clouds. Higher ratios of particle concentrations greater than 3 versus 10 nm (N_3/N_{10}) were mainly observed above boundary layer cloud tops during winter as compared to summer. Cold dry air and low aerosol surface area concentration facilitate NPF over the ACTIVATE region; these conditions are especially prevalent during flights coinciding with cold air outbreaks.

Plain Language Summary Airborne data collected during the Aerosol Cloud meTeorology Interactions oVer the western ATlantic Experiment (ACTIVATE) campaign's first year of research flights during the winter (February 14 to March 12, 2020) and summer (August 13 to September 30, 2020) provide insight on new particle formation over the Western North Atlantic Ocean. The formation of new particles in the atmosphere is the primary contributor to total particle number concentration and plays a key role in the cloud condensation nuclei budget. Airborne observations reveal more active new particle formation during the winter than summer, especially just above boundary layer cloud tops. Influential conditions coinciding with new particle formation include cold and dry air, along with low aerosol surface area concentration and high levels of precursor gases from continental outflow. These conditions are shown to be most prevalent during cold air outbreaks in the winter off the United States East Coast.

1. Introduction

New particle formation (NPF) is the dominant contributor to total particle number concentration and significantly impacts the cloud condensation nuclei (CCN) budget (Kerminen et al., 2018; Merikanto et al., 2009). NPF occurs in diverse regions, ranging across urban, remote, and Arctic and polar areas (Kerminen et al., 2018; Schmale & Baccarini, 2021; Sellegri et al., 2019, and references therein). NPF has been observed in the boundary layer (BL) when influenced by biogenic (Häkkinen et al., 2013; Zhao et al., 2020) and anthropogenic sources (e.g., Siebert et al., 2004), in the free troposphere (FT; 3,000–15,000 m) where low temperatures and cloud processes provide favorable conditions for NPF (Clarke et al., 2013), and at the interface between the BL and FT (Dadashazar et al., 2018; Siebert et al., 2004). Several studies have also reported NPF in the lower FT (~4,000 m) primarily driven by upward transport from the BL (Bianchi et al., 2016) or convective movement. In contrast to long-term ground-based studies (e.g., Kristensson et al., 2014; Kulmala et al., 2004), airborne measurements provide a three-dimensional spatial perspective on NPF (Croft et al., 2021; McCoy et al., 2021; Rose et al., 2015; Weber et al., 1998). Airborne measurements in marine regions show that NPF occurs preferentially in the FT compared to the marine BL (Sanchez et al., 2018; Williamson et al., 2019), predominantly in tropical convective regions and cloud outflow areas (Clarke & Kapustin, 2002; Waddicor et al., 2012). Among the knowledge gaps identified for NPF are the role of clouds in free-tropospheric NPF and processes involved at the interface between the BL

and the FT (Kerminen et al., 2018). Since nucleated particles impact the CCN budget and clouds themselves can influence NPF (Hegg, 1990; Kerminen & Wexler, 1994; Zheng et al., 2021), it is necessary to study NPF in the vicinity of clouds to advance understanding of aerosol-cloud interactions that are associated with the largest uncertainty in total anthropogenic radiative forcing (IPCC, 2013).

The Aerosol Cloud meTeorology Interactions oVer the western ATlantic Experiment (ACTIVATE) provides airborne data ideal for studying NPF around clouds due to a flight approach centered around accumulating a high volume of data around marine boundary layer clouds. More details about the ACTIVATE campaign are described in Sorooshian et al. (2019). Zheng et al. (2021) found that low particle concentration and temperature, in addition to readily available precursor gases after the passage of cold fronts, create favorable conditions for NPF. Studies in the Finnish boreal forest showed that NPF is related to cold air advection behind cold fronts (Nilsson et al., 2001a, 2001b). Cold air outbreaks (CAOs) are frequently occurring extreme events over land and oceans extending from the tropics to the polar regions in both the northern and southern hemispheres (Smith & Sheridan, 2020). Conveniently, CAOs are a key feature of the Western North Atlantic Ocean (WNAO) region. CAOs give rise to shallow cumulus clouds (postfrontal clouds) that are poorly treated by climate models (Rémillard & Tselioudis, 2015). Improving understanding of potential NPF characteristics in CAOs is helpful owing to the importance of aerosol size distributions in influencing cloud properties. This study uses ACTIVATE data to address NPF features, like seasonal and spatial statistics, along with influential factors in and around clouds, including in postfrontal conditions associated with CAOs.

2. Data

ACTIVATE involves two aircraft (HU-25 Falcon and King Air) flying in a systematic and coordinated way such that the Falcon acquires in situ data in the BL (<2,500 m) and the King Air simultaneously flies at 8,000–10,000 m providing remote sensing data for aerosol particles and clouds in the same vertical column. We focus on Falcon data, which were collected in "ensembles" comprised of the following level leg types when clouds were present: MinAlt cloudy = minimum flight altitude in cloudy conditions, BCB = below cloud base, ACB = above cloud base, BCT = below cloud top, ACT = above cloud top. Ensembles in cloud-free conditions included: MinAlt clear = minimum flight altitude in clear conditions, BBL = below boundary layer top, and ABL = above boundary layer top. An idealized depiction of the Falcon's nominal flight pattern in clear and cloudy conditions is shown in Figure S1 in Supporting Information S1.

We use available data from the winter (February 14 to March 12, 2020; n = 96,434) and summer (August 13 to September 30, 2020; n = 70,827) deployments of ACTIVATE's first year of flights. Additional details about the flights and data are in Section S1 in Supporting Information S1. We use the following data: particle concentrations greater than 3 and 10 nm from Condensation Particle Counter (CPC) instruments (TSI-3776; D_p > 3 nm [N_3] and TSI-3772; D_p > 10 nm [N_{10}]); total area surface concentration (S_{Tot}) from a Laser Aerosol Spectrometer (LAS; TSI Model 3340; 100.0–3162.3 nm midpoint diameter); ultrafine and Aitken mode particle size distributions from a Scanning Mobility Particle Sizer (SMPS; TSI 3085 Nano DMA and TSI 3776 CPC; 3.2–89.1 nm midpoint diameter); static air temperature (Rosemount 102); relative humidity (RH) from the Diode Laser Hygrometer (DLH; Diskin et al., 2002); ozone (O_3) from a dual-beam photometer (2B Technologies Model 205); and carbon monoxide (CO) from a Picarro G2401 gas concentration analyzer (DiGangi et al., 2021). Sulfur dioxide (SO_2) concentrations along the Falcon flight path were obtained from the Modern-Era Retrospective analysis for Research and Applications-Version 2 (MERRA-2; Gelaro et al., 2017). All data except SMPS (~45 s resolution) are at 1-s resolution. The MERRA-2 data were retrieved at an interval of 30 s.

To eliminate artifacts from cloud droplet shattering, in-cloud data were used only when liquid water content was <0.02 g m^{-3} (Fast Cloud Droplet Probe, FCDP; 3–50 μm; Stratton Park Engineering Company Incorporated (SPEC Inc.); Knop et al., 2021). Data from the High Spectral Resolution Lidar (HSRL-2) aboard the King Air are used for cloud top heights (CTH). The Hybrid Single-Particle Lagrangian Integrated Trajectory (HYSPLIT; Rolph et al., 2017; Stein et al., 2015) model was used to identify air mass transport pathways arriving at points along flight tracks. Those 24 and 48-hr back trajectories were based on Global Data Assimilation System (GDAS) meteorological data (0.5° × 0.5°) and calculated every 6 hr.

Table 1
Cumulative Distribution Function Probabilities for the Winter and Summer Falcon Legs

		Winter probability (%)			Summer probability (%)		
Ensemble type	Legs	≥1.3	≥1.5	≥1.8	≥1.3	≥1.5	≥1.8
Cloudy	MinAlt	26.60	0.95	0.01	3.90	0.02	0
	BCB	40.70	1.52	0.01	9.30	0.06	0
	ACB	45.09	2.86	0.03	21.06	0.85	0.01
	BCT	59.78	11.54	0.51	26.72	1.15	0.02
	ACT	73.97	35.33	7.34	42.31	1.83	0.01
Clear	MinAlt	54.79	21.10	3.73	3.75	0.02	0
	BBL	58.08	21.30	3.27	7.44	0.03	0
	ABL	39.92	5.66	0.15	12.16	0.08	0

Note. Probabilities are reported in percentages to report a N_3/N_{10} greater or equal to 1.3, 1.5, and 1.8.

3. Results and Discussion

3.1. Seasonal Comparison

Similar to early studies leveraging differences between CPCs with varying minimum diameters (e.g., Clarke, 1993; Covert et al., 1992; Weber et al., 1998), we use the ratio between particle concentrations greater than 3 and 10 nm (N_3/N_{10}) to provide evidence of NPF. Although small in size, newly formed particles can continue to grow into the Aitken mode and subsequently contribute to the CCN budget and more directly impact climate (e.g., Wang et al., 2021). Three threshold ratio values are first considered here (1.3/1.5/1.8) chosen to be comfortably above unity and with sufficient spacing to quantify different degrees of NPF. We caution at the outset that enhanced ratios above unity indicate the presence of nucleated particles and not necessarily that the NPF occurred at the point of sampling. Winter data exhibited higher probabilities of $N_3/N_{10} \geq 1.3/1.5/1.8$ regardless of leg type (Table 1); associated cumulative distribution function results are in Figure S2 in Supporting Information S1. ACT legs exhibited the highest probabilities of $N_3/N_{10} \geq 1.3$ (winter = 73.97%, summer = 42.31%) followed by BCT legs (winter = 59.78%, summer = 26.72%). Noteworthy was that ACB legs ranked third and fifth in summer (21.06%) and winter (45.09%), respectively. MinAlt cloudy legs show the lowest probabilities for $N_3/N_{10} \geq 1.3$ during the winter (26.90%) and the second lowest in summer (3.90%) likely due to some combination of high aerosol surface area from surface sea spray emissions and, in the case of cloudy conditions, suppressed NPF with lower incident solar radiation beneath the cloud (Dada et al., 2017). Probabilities for ratios ≥1.5 and 1.8 are also the highest for ACT levels in winter and summer. Leg probabilities during summer for ratios greater than 1.8 are likely not statistically different from zero. Therefore, winter and near-cloud conditions are favorable for high N_3/N_{10}.

As ACT legs show the highest probabilities of enhanced N_3/N_{10}, statistics for parameters potentially relevant to NPF are compared between winter and summer (Figure 1). Descriptive statistics for N_3/N_{10} values can be found in Table S1 in Supporting Information S1. There was an insignificant change in the difference (dH) between ACT leg altitudes and respective CTHs between seasons (winter/summer = 270/350 m; Figure S3 in Supporting Information S1). While absolute concentrations of N_3 and N_{10} are lower in winter, N_3/N_{10} (1.41) is higher coincident with lower wintertime median values (winter/summer) of S_{Tot} (8.67/10.34 μm^2 cm^{-3}), air temperature

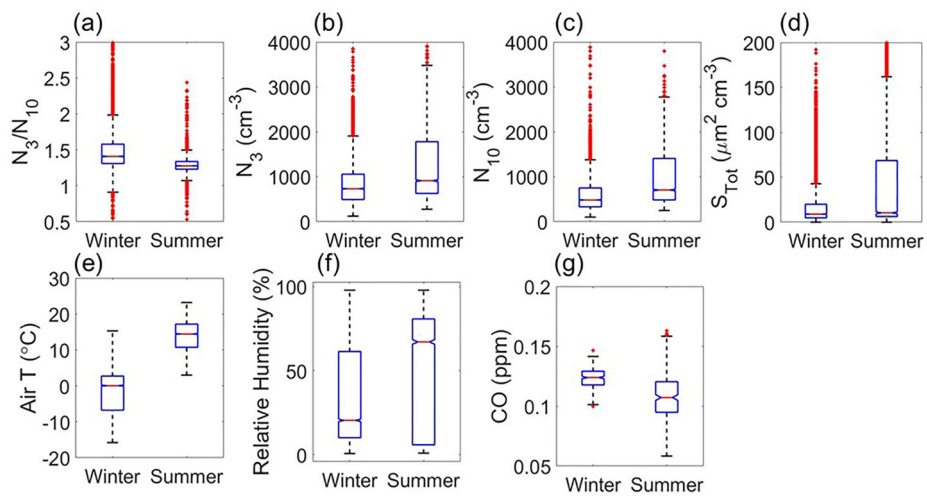

Figure 1. Box notched plot comparison between the winter and summer research flights for above cloud top (ACT) legs. Red solid line represents the median. Box edges show the 75th and 25th percentiles. The upper and lower whiskers represent the upper limit (third quartile (Q3) + 1.5 × interquartile range) and lower limit (first quartile (Q1) – 1.5 × interquartile range), respectively. The red markers show outliers greater than 1.5 × the interquartile range below Q1 or above Q3. The notch marks the 95% confidence interval for the median.

(0.07/14.44 °C), and RH (20.40/67.10%), along with higher CTH (1,500/800 m) and CO (0.12/0.11 ppm). A significant difference ($p < 0.05$; Mann-Whitney test) was determined for the aforementioned parameters (except dH) between winter and summer.

An inverse relationship between the N_3/N_{10} and S_{Tot} is observed for the winter ACT legs with S_{Tot} median values comparable to S_{Tot} values reported in the FT (Zheng et al., 2021). This inverse relation is well documented in previous studies (Clarke et al., 1998; Perry & Hobbs, 1994; Zheng et al., 2021). The relationship between temperature and NPF may be ambiguous as several temperature-related processes may enhance or hinder NPF (Kerminen et al., 2018; and references therein). ACTIVATE data reveal elevated N_3/N_{10} associated with low temperatures (winter). This observation is consistent with previous field study in the Eastern North Atlantic (Zheng et al., 2021) and controlled chamber experiments (Kürten et al., 2016). In contrast to winter data, summer data exhibit a lower N_3/N_{10} median (1.28). The summer S_{Tot} median (10.34 μm^2 cm^{-3}) is similar to the winter median (8.67 μm^2 cm^{-3}) and values from other studies (Clarke, 1993; Zheng et al., 2021). However, summer data reveal higher median temperature (14.44 °C) and RH (67.10%) suggesting that higher wintertime ratios may occur because of the combination of low S_{Tot}, temperature, and RH.

ACTIVATE winter data were also characterized by lower RH. NPF has been linked to both lower RH conditions (Cai et al., 2017) due to increased solar radiation and gas-phase oxidation chemistry (Li et al., 2019) and higher RH attributed to inhibition of terpene ozonolysis reactions that lead to NPF (Bonn & Moortgat, 2003; Hyvönen et al., 2005). Regarding CO, Zheng et al. (2021) observed a positive relation between CO and N_3/N_{10} in the upper decoupled layer of the marine BL while Jeong et al. (2006) concluded that anthropogenic emissions into cold air promote NPF over eastern North America.

3.2. Above Cloud Top Data Analysis During Winter

Evidence of NPF above the cloud tops is observed frequently over the WNAO. Previous studies have reported an enhancement of total (Hegg et al., 1991; Hudson & Frisbie, 1991) and sub-10 nm (Weber et al., 2001) particle number concentrations around cloud edges when compared to areas farther away from clouds or in clouds. These observations range in altitude from the BL to several kilometers in the FT in both marine and continental atmospheres. Increased ultraviolet irradiance and turbulence surrounding clouds have previously been linked to NPF above cloud top (e.g., Weber et al., 2001; Wehner et al., 2015).

A comparison between the ACT and ABL legs provides insight on the potential importance of clouds for NPF. Both legs are above the BL with the main difference being the presence of cloud in ACT legs compared to cloud-free conditions during ABL legs. Higher probabilities of $N_3/N_{10} \geq 1.3$ were observed during the ACT legs compared to the ABL legs. Even though this study cannot provide definite proof, the results at least support clouds playing an important role in NPF by the redistribution of precursor vapors by convective clouds and enhanced actinic flux above clouds (Clarke et al., 1998; Rose et al., 2015). Furthermore, this comparison counters the notion that enhanced N_3/N_{10} values offshore above the BL are due primarily to transport of air enriched with nucleated particles from land.

To gain more insight into winter ACT leg results, data were separated into "low" and "high" N_3/N_{10} groups based on leg-mean N_3/N_{10} being below and above the 25th and 75th percentile, respectively (Figure 2). The high N_3/N_{10} data group expectedly exhibited higher median ratios (1.69) associated with lower median temperature and RH (−4.66 °C, 20.91%) and lower S_{Tot} (8.97 μm^2 cm^{-3}) compared to the low N_3/N_{10} group (1.29) with higher median values of the aforementioned parameters (3.01 °C, 61.99%, 29.25 μm^2 cm^{-3}).

HYSPLIT 24-hr back trajectories support the hypothesis that winter ACT legs' air masses are influenced by transport of anthropogenic air from the continental U.S. (Figure S4 in Supporting Information S1). We identify trajectories coming from two clusters, one from the north/northwest ("north") and the other from the west/northwest ("west") for the high and low N_3/N_{10} groups. The two clusters (west versus north) are compared for the high N_3/N_{10} group only as the difference in median N_3/N_{10} for the west and north clusters in the low group was negligible (1.29 versus 1.30). For the high N_3/N_{10} group, back trajectories coming from the west (Figure S5 in Supporting Information S1) show higher median N_3/N_{10} (1.91) along with lower median values of S_{Tot} (5.60 μm^2 cm^{-3}) and RH (14.43%) when compared to northerly trajectories (1.66, 11.18 μm^2 cm^{-3}, 24.25%). Although air temperature was higher in the west cluster (−4.59 °C versus −7.76 °C), it was still very cold and thus, that difference between clusters may have been uninfluential for NPF.

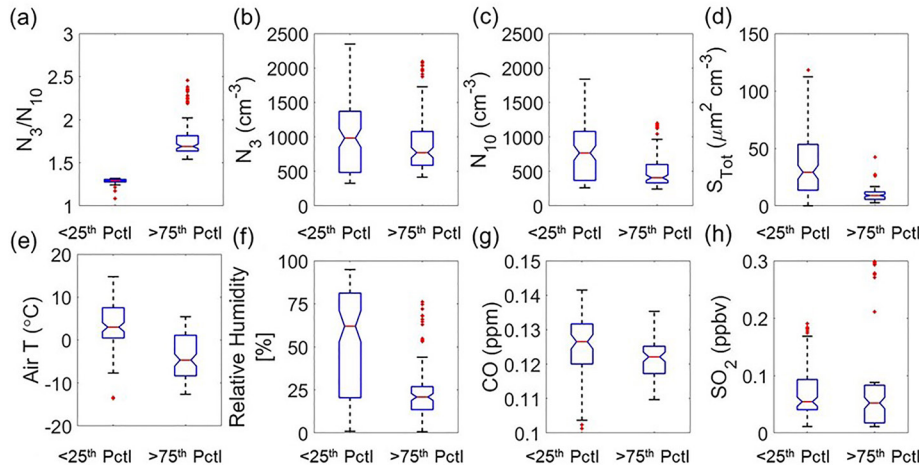

Figure 2. Same as Figure 1 except for N_3/N_{10} below the 25th percentile and above the 75th percentile (pctl) for winter 2020 above cloud top (ACT) legs.

The west group exhibited a slightly lower CO concentrations median (0.12 ppm) compared to the low group (0.13 ppm) with the values being statistically different ($p < 0.05$; Mann-Whitney test). A lower SO_2 median is also found for the west cluster (0.017 versus 0.083 ppbv). This is consistent with earlier studies that have reported low concentrations of ambient SO_2 during NPF events (e.g., Dai et al., 2017). In contrast, other studies have reported that high SO_2 concentrations lead to favorable NPF conditions (e.g., Birmili & Wiedensohler, 2000). The delicate balance between the variables that favor and hinder NPF downwind larger SO_2 sources might explain these conflicting results. Furthermore, it may be that sufficient gaseous precursors are present even in the west cluster and that the more important factors could be other environmental conditions such as lower S_{Tot}. Figure S6 in Supporting Information S1 shows an inverse relationship between N_3/N_{10} and both S_{Tot} and temperature for the winter ACT legs. Previous work (Zheng et al., 2021) defined a threshold over which NPF is inhibited under different cloud conditions (clear, scattered, and overcast). An increased N_3/N_{10} in the marine BL was only observed when S_{Tot} was less than 10 $\mu m^2\ cm^{-3}$ (Zheng et al., 2021). Our data do not reveal a threshold for S_{Tot} at which NPF is hindered for different leg types. Combined ACTIVATE data from 2020 and subsequent years of flights (2021 and 2022) will provide a more solid statistical foundation to address this question.

Using HYSPLIT trajectories, we analyze the accumulated precipitation along trajectories (APT) arriving at ACT legs to determine if there was a relationship between potential wet removal and low S_{Tot} in ACT air masses (Figure S7 in Supporting Information S1). Our analysis did not find a significant relationship between the two parameters. However, a previous study has associated cumulus drizzle and precipitation with lower S_{Tot} due to the removal of large particles in the upper decoupled layer of the marine BL (Zheng et al., 2021). Therefore, we conclude that the west cluster is linked to the main factors already shown to promote high N_3/N_{10} (i.e., lower S_{Tot} and RH). The WNAO experiences frequent passage of cold fronts in the winter, which can induce prominent low-level CAOs across the coastal waters. Conditions typical of cold fronts like low S_{Tot}, cold temperature, and high actinic fluxes between the scattered clouds in the upper part of the remote marine BL are favorable for NPF (Zheng et al., 2021).

4. Case Studies

Here we probe deeper into two case flights from the winter 2020 campaign characterized by high N_3/N_{10} above BL cloud tops. We use data from ACTIVATE Research Flight 10 (RF10; first aircraft launch (i.e., flight 1)) on February 28, 2020 and RF17 (second aircraft launch (i.e., flight 2)) on March 8, 2020. RFs 10 and 17 differ in their synoptic setup but show the characteristic cloud streets frequently formed in strong CAOs as evident from satellite imagery (Figure 3a and Figure S8a in Supporting Information S1). On February 28, 2020, the flight region was dominated by a deep trough over the eastern U.S. and a surface low pressure system in southeastern Canada, with a cold front located well offshore. RF17 on March 8, 2020 was characterized by strong surface high pressure over the eastern U.S. downstream of an upper-level ridge in the central U.S. Both flight days were

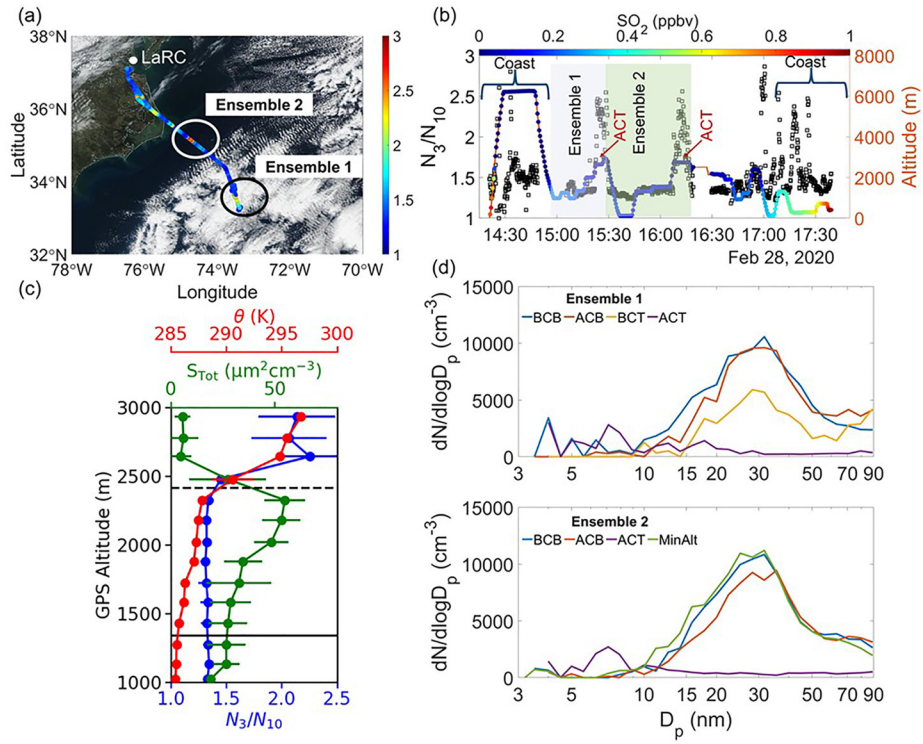

Figure 3. Results from Aerosol Cloud meTeorology Interactions oVer the western ATlantic Experiment (ACTIVATE) RF10 (February 28, 2020): (a) HU-25 Falcon flight path overlaid on Visible Infrared Imaging Radiometer Suite (VIIRS) imagery (NASA Worldview) with N_3/N_{10} as the color bar. Black and white circles show the approximate location of ensembles 1 and 2, respectively. (b) Time series of N_3/N_{10} (black markers) and aircraft altitude (colored by the MERRA-2 SO_2). Shaded regions represent individual cloud ensembles. (c) Vertical profiles of potential temperature, S_{Tot}, and N_3/N_{10} based on data from the descent connecting the above cloud top (ACT) and MinAlt leg during cloud ensemble 1 (15:22:37–15:36:37). Black solid and dashed lines represent cloud base and top heights, respectively. (d) SMPS aerosol number size distributions for different level legs in cloud ensembles 1 and 2.

visually identified as having CAO conditions (Seethala et al., 2021) and using dropsondes deployed from the King Air following the method described in Papritz et al. (2015).

These two case flights had common characteristics promoting NPF: cold and dry conditions, low S_{Tot}, and the presence of precursor gases from continental outflow. This is consistent with previous studies that have reported NPF under CAOs conditions (e.g., Lee et al., 2008). RF10's N_3/N_{10} in the two ACT legs (Figures 3a and 3b) are 2.25 (15:22:22–15:26:36) and 1.91 (16:07:52–16:16:39), respectively. The N_3/N_{10} vertical profile shows an inverse relation with S_{Tot} and a positive relationship with potential temperature (θ; Figure 3c). High N_3/N_{10} values (≥1.3) were also observed closer to the shore in cloud-free conditions after take-off (900–6,300 m) and during the transit leg at 6,300 m (Figure 3b). Considering that high N_3/N_{10} values are reported at different altitudes, we speculate that enhanced coastal values were aided by higher concentrations of precursor gases (e.g., SO_2) closer to the continental sources as compared to farther offshore (O'Dowd & Hoffmann, 2006). MERRA-2 SO_2 and in situ O_3 concentrations along the path for RF10 (Figures S9a and S9b in Supporting Information S1) are consistent with North American pollution outflow with maximum levels along the coast and a gradual reduction eastward due to dilution. SO_2 concentrations in the ACT legs were not as high as concentrations in legs by the coast, highlighting that if the S_{Tot} is sufficiently low, NPF can occur even at low concentrations of SO_2 (Covert et al., 1992) or other reactive gases (e.g., dimethyl sulfide; Zheng et al., 2021). Alternatively, NPF may have occurred closer to land and the air masses were transported to the sampled ACT areas where enhanced ratios were observed.

Vertically resolved particle size distributions show clearly that only the ACT legs had pronounced number concentrations between 3 and 10 nm (Figure 3d), indicative of the majority of NPF occurring aloft and not in or below the cloud layer. Similar to RF10, RF17 data revealed median N_3/N_{10} above 1.3 with values of 1.64 and 1.56 in ACT legs for ensembles 1 and 2, respectively (Figures S8a and S8b in Supporting Information S1). The particle

size distribution data also confirm elevated concentrations of sub-10 nm particles in the ACT legs (Figure S8d in Supporting Information S1) compared to the lower altitude legs. Consistent with data reported for RF10, the SO_2 (MERRA-2) and O_3 (in situ) concentrations for RF17 show higher values near the coast and a decrease farther into the WNAO (Figures S9c and S9d in Supporting Information S1).

5. Conclusions

This study provides a first look at NPF over the ACTIVATE region with airborne data in winter and summer. Seasonal analysis of N_3/N_{10} statistics indicates that NPF is more prevalent off the U.S. East Coast in winter rather than summer. Probabilities of high N_3/N_{10} ($\geq$1.3/1.5/1.8) peak above cloud top regardless of season when compared to other vertical levels. Conditions typical of CAOs like low temperature, dry conditions, and continental outflow with NPF precursor gases, along with low S_{Tot}, are favorable for NPF in the ACTIVATE region. Limitations of this study are the lack of in situ precursor concentration measurements, for which reanalysis data were used instead.

Our results cannot unambiguously diagnose all details of NPF in the study region, including details associated with cloud influence on NPF and whether the initial nucleation occurs more over land or ocean, with the former implying that the high observed ratios in this work are due to transport rather than actual nucleation in the vicinity of the airborne measurements. This effort requires more detailed analysis of aerosol size distribution evolution and transport modeling, which can benefit from more statistics as ACTIVATE flights continue in the same region in 2021 and 2022. Future work will look more into aerosol growth dynamics from 3 to 10 nm and the influence of other relevant parameters affecting NPF in the ACTIVATE region such as actinic flux, especially as high N_3/N_{10} are observed immediately above BL cloud tops. ACTIVATE has the advantage of having the King Air flying above clouds to remotely measure aerosol particles and clouds using the High Spectral Resolution Lidar-2 and the Research Scanning Polarimeter, which potentially opens new avenues for NPF-related research. Lastly, model simulations of post-frontal cloud evolution associated with CAOs can benefit from these results as nucleated particles impact the CCN budget and cloud properties.

Conflict of Interest

The authors declare no conflicts of interest relevant to this study.

Data Availability Statement

MERRA-2 data are available at https://doi.org/10.5067/LTVB4GPCOTK2 and ACTIVATE airborne data can be accessed from http://doi.org/10.5067/ASDC/ACTIVATE_Aerosol_AircraftInSitu_Falcon_Data_1. ACTIVATE data can be accessed by registering for an Earthdata account/login: https://urs.earthdata.nasa.gov/. All dataIDs begin with "ACTIVATE." DataIDs included "Microphysical," "Summary," "TraceGas-O3," "LegFlags," "FCDP," "DLH-H_2O," and "SMPS.".

Acknowledgments
We acknowledge funding from NASA Grant 80NSSC19K0442 in support of ACTIVATE, a NASA Earth Venture Suborbital-3 (EVS-3) investigation funded by NASA's Earth Science Division and managed through the Earth System Science Pathfinder Program Office. C. V. and S. K. thank funding by the DFG (German Research Foundation)-TRR301-Project-ID 428312742 and SPP1294 HALO under contract VO1504/7-1. The authors gratefully acknowledge the NOAA Air Resources Laboratory for the provision of the HYSPLIT transport and dispersion model and READY website (http://ready.arl.noaa.gov). We recognize the use of imagery from the NASA Worldview application (https://worldview.earthdata.nasa.gov/), part of the NASA Earth Observing System Data and Information System. We wish to thank the pilots and aircraft maintenance personnel of NASA Langley Research Services Directorate for their work in conducting the ACTIVATE flights.

References

Bianchi, F., Trostl, J., Junninen, H., Frege, C., Henne, S., Hoyle, C. R., et al. (2016). New Particle Formation in the free troposphere: A question of chemistry and timing, *Science*, *352*(6289), 1109–1112. https://doi.org/10.1126/science.aad5456

Birmili, W., & Wiedensohler, A. (2000). New particle formation in the continental boundary layer: Meteorological and gas phase parameter influence. *Geophysical Research Letters*, *27*(20), 3325–3328. https://doi.org/10.1029/1999GL011221

Bonn, B., & Moortgat, G. K. (2003). Sesquiterpene ozonolysis: Origin of atmospheric new particle formation from biogenic hydrocarbons. *Geophysical Research Letters*, *30*(11), 1585. https://doi.org/10.1029/2003GL017000

Cai, R., Yang, D., Fu, Y., Wang, X., Li, X., Ma, Y., et al. (2017). Aerosol surface area concentration: A governing factor in new Particle Formation in Beijing. *Atmospheric Chemistry and Physics*, *17*(20), 12327–12340. https://doi.org/10.5194/acp-17-12327-2017

Clarke, A. D. (1993). Atmospheric nuclei in the Pacific midtroposphere: Their nature, concentration, and evolution. *Journal of Geophysical Research*, *98*(D11), 20633–20647. https://doi.org/10.1029/93JD00797

Clarke, A. D., Freitag, S., Simpson, R., Hudson, J. G., Howell, S. G., Brekhovskikh, V. L., et al. (2013). Free troposphere as a major source of CCN for the equatorial pacific boundary layer: Long-range transport and teleconnections. *Atmospheric Chemistry and Physics*, *13*(15), 7511–7529. https://doi.org/10.5194/acp-13-7511-2013

Clarke, A. D., & Kapustin, V. N. (2002). A pacific aerosol survey. Part I: A decade of data on particle production, transport, evolution, and mixing in the troposphere. *Journal of the Atmospheric Sciences*, *59*(3), 363–382. https://doi.org/10.1175/1520-0469(2002)059<0363:APASPI>2.0.CO;2

Clarke, A. D., Varner, J. L., Eisele, F., Mauldin, R. L., Tanner, D., & Litchy, M. (1998). Particle production in the remote marine atmosphere: Cloud outflow and subsidence during ACE 1. *Journal of Geophysical Research*, *103*(D13), 16397–16409. https://doi.org/10.1029/97JD02987

Covert, D. S., Kapustin, V. N., Quinn, P. K., & Bates, T. S. (1992). New particle formation in the marine boundary layer. *Journal of Geophysical Research*, *97*(D18), 20581–20589. https://doi.org/10.1029/92JD02074

Croft, B., Martin, R. V., Moore, R. H., Ziemba, L. D., Crosbie, E. C., Liu, H., & et al. (2021). Factors controlling marine aerosol size distributions and their climate effects over the northwest Atlantic Ocean region. *Atmospheric Chemistry and Physics*, *21*(3), 1889–1916. https://doi.org/10.5194/acp-21-1889-2021

Dada, L., Paasonen, P., Nieminen, T., Buenrostro Mazon, S., Kontkanen, J., Peräkylä, O., et al. (2017). Long-term analysis of clear-sky new particle formation events and nonevents in Hyytiälä. *Atmospheric Chemistry and Physics*, *17*(10), 6227–6241. https://doi.org/10.5194/acp-17-6227-2017

Dadashazar, H., Braun, R. A., Crosbie, E., Chuang, P. Y., Woods, R. K., Jonsson, H. H., & Sorooshian, A. (2018). Aerosol characteristics in the entrainment interface layer in relation to the marine boundary layer and free troposphere. *Atmospheric Chemistry and Physics*, *18*(3), 1495–1506. https://doi.org/10.5194/acp-18-1495-2018

Dai, L., Wang, H., Zhou, L., An, J., Tang, L., Lu, C., et al. (2017). Regional and local new particle formation events observed in the Yangtze River Delta region, China. *Journal of Geophysical Research: Atmospheres*, *122*, 2389–2402. https://doi.org/10.1002/2016JD026030

DiGangi, J. P., Choi, Y., Nowak, J. B., Halliday, H. S., Diskin, G. S., Feng, S., et al. (2021). *Seasonal variability in local carbon dioxide combustion sources over the central and eastern US using airborne in-situ enhancement ratios*.Earth and Space Science Open Archive ESSOAr.

Diskin, G. S., Podolske, J. R., Sachse, G. W., & Slate, T. A. (2002). Open-path airborne tunable diode laser hygrometer. Paper presented at Diode lasers and applications in atmospheric sensing. International Society for Optics and Photonics. https://doi.org/10.1117/12.453736

Gelaro, R., McCarty, W., Suarez, M. J., Todling, R., Molod, A., Takacs, L., et al. (2017). The Modern-Era Retrospective analysis for research and applications, version 2 (MERRA-2). *Journal of Climate*, *30*(13), 5419–5454. https://doi.org/10.1175/jcli-d-16-0758.1

Häkkinen, S., Manninen, H., Yli-Juuti, T., Merikanto, J., Kajos, M., Nieminen, T., et al. (2013). Semi-empirical parameterization of size-dependent atmospheric nanoparticle growth in continental environments. *Atmospheric Chemistry and Physics*, *13*(15), 7665–7682.

Hegg, D. A. (1990). Heterogeneous production of cloud condensation nuclei in the marine atmosphere. *Geophysical Research Letters*, *17*(12), 2165–2168. https://doi.org/10.1029/GL017i012p02165

Hegg, D. A., Radke, L. F., & Hobbs, P. V. (1991). Measurements of Aitken nuclei and cloud condensation nuclei in the marine atmosphere and their relation to the DMS-cloud-climate hypothesis. *Journal of Geophysical Research: Atmospheres*, *96*(D10), 18727–18733. https://doi.org/10.1029/91JD01870

Hudson, J. G., & Frisbie, P. R. (1991). Cloud condensation nuclei near marine stratus. *Journal of Geophysical Research*, *96*(D11), 20795–20808. https://doi.org/10.1029/91JD02212

Hyvönen, S., Junninen, H., Laakso, L., Maso, M. D., Grönholm, T., Bonn, B., & Pohja, T. (2005). A look at aerosol formation using data mining techniques. *Atmospheric Chemistry and Physics*, *5*(12), 3345–3356.

IPCC. (2013). *Climate change 2013: The physical science basis* (p. 1535). Cambridge University Press.

Jeong, C. H., Evans, G. J., Hopke, P. K., Chalupa, D., & Utell, M. J. (2006). Influence of atmospheric dispersion and new particle formation events on ambient particle number concentration in Rochester, United States, and Toronto, Canada. *Journal of the Air & Waste Management Association*, *56*(4), 431–443. https://doi.org/10.1080/10473289.2006.10464519

Kerminen, V. M., Chen, X.M., Vakkari, V., Petaja, T., Kulmala, M., & Bianchi, F. (2018). Atmospheric new Particle Formation and growth: Review of field observations. *Environmental Research Letters*, *13*(10), 103003. https://doi.org/10.1088/1748-9326/aadf3c

Kerminen, V. M., & Wexler, A. S. (1994). Particle formation due to SO_2 oxidation and high relative humidity in the remote marine boundary layer. *Journal of Geophysical Research: Atmospheres*, *99*(D12), 25607–25614. https://doi.org/10.1029/94JD01988

Knop, I., Bansmer, S. E., Hahn, V., & Voigt, C. (2021). Comparison of different droplet measurement techniques in the Braunschweig Icing Wind Tunnel. *Atmospheric Measurement Techniques*, *14*(2), 1761–1781. https://doi.org/10.5194/amt-14-1761-2021

Kristensson, A., Johansson, M., Swietlicki, E., Kivekäs, N., Hussein, T., Nieminen, T., et al. (2014). NanoMap: Geographical mapping of atmospheric new-particle formation through analysis of particle number size distribution and trajectory data. *Boreal Environment Research*, *19*, 329–342.

Kulmala, M., Vehkamäki, H., Petäjä, T., Dal Maso, M., Lauri, A., Kerminen, V. M., et al. (2004). Formation and growth rates of ultrafine atmospheric particles: A review of observations. *Journal of Aerosol Science*, *35*(2), 143–176. https://doi.org/10.1016/j.jaerosci.2003.10.003

Kürten, A., Bianchi, F., Almeida, J., Kupiainen-Määttä, O., Dunne, E. M., Duplissy, J., et al. (2016). Experimental particle formation rates spanning tropospheric sulfuric acid and ammonia abundances, ion production rates, and temperatures, *Journal of Geophysical Research: Atmospheres*, *121*, 12377–12400. https://doi.org/10.1002/2015JD023908

Lee, Y.-G., Lee, H.-W., Kim, M.-S., Choi, C. Y., & Kim, J. (2008). Characteristics of particle formation events in the coastal region of Korea in 2005. *Atmospheric Environment*, *42*(16), 3729–3739. https://doi.org/10.1016/j.atmosenv.2007.12.064

Li, X., Chee, S., Hao, J., Abbatt, J. P. D., Jiang, J., & Smith, J. N. (2019). Relative humidity effect on the formation of highly oxidized molecules and new particles during monoterpene oxidation. *Atmospheric Chemistry and Physics*, *19*(3), 1555–1570. https://doi.org/10.5194/acp-19-1555-2019

McCoy, I.L., Bretherton, C. S., Wood, R., Twohy, C. H., Gettelman, A., Bardeen, C. G., & Toohey, D. W. (2021). Influences of recent particle formation on southern ocean aerosol variability and low cloud properties. *Journal of Geophysical Research: Atmospheres*, *126*, e2020JD033529. https://doi.org/10.1029/2020JD033529

Merikanto, J., Spracklen, D., Mann, G., Pickering, S., & Carslaw, K. (2009). Impact of nucleation on global CCN. *Atmospheric Chemistry and Physics*, *9*(21), 8601–8616. https://doi.org/10.5194/acp-9-8601-2009

Nilsson, E. D., Paatero, J., & Boy, M. (2001). Effects of air masses and synoptic weather on aerosol formation in the continental boundary layer. *Tellus B: Chemical and Physical Meteorology*, *53*(4), 462–478. https://doi.org/10.3402/tellusb.v53i4.16619

Nilsson, E. D., Rannik, Ü., Kumala, M., Buzorius, G., & O'dowd, C. D. (2001). Effects of continental boundary layer evolution, convection, turbulence and entrainment, on aerosol formation. *Tellus B: Chemical and Physical Meteorology*, *53*(4), 441–461. https://doi.org/10.3402/tellusb.v53i4.16617

O'Dowd, C. D., & Hoffmann, T. (2006). Coastal new Particle Formation: A review of the current state-of-the-art. *Environmental Chemistry*, *2*(4), 245–255.

Papritz, L., Pfahl, S., Sodemann, H., & Wernli, H. (2015). A climatology of cold air outbreaks and their impact on air–sea heat fluxes in the high-latitude South Pacific. *Journal of Climate*, *28*(1), 342–364. https://doi.org/10.1175/JCLI-D-14-00482.1

Perry, K. D., & Hobbs, P. V. (1994). Further evidence for particle nucleation in clear air adjacent to marine cumulus clouds. *Journal of Geophysical Research*, *99*(D11), 22803–22818. https://doi.org/10.1029/94JD01926

Rémillard, J., & Tselioudis, G. (2015). Cloud regime variability over the Azores and its application to climate model evaluation. *Journal of Climate*, *28*(24), 9707–9720.

Rolph, G., Stein, A., & Stunder, B. (2017). Real-time environmental applications and Display sYstem: READY. *Environmental Modelling & Software*, *95*, 210–228. https://doi.org/10.1016/j.envsoft.2017.06.025

Rose, C., Sellegri, K., Freney, E., Dupuy, R., Colomb, A., Pichon, J.-M., et al. (2015). Airborne measurements of new particle formation in the free troposphere above the Mediterranean Sea during the HYMEX campaign. *Atmospheric Chemistry and Physics*, *15*(17), 10203–10218. https://doi.org/10.5194/acp-15-10203-2015

Sanchez, K. J., Chen, C.-L., Russell, L. M., Betha, R., Liu, J., Price, D. J., et al. (2018). Substantial seasonal contribution of observed biogenic sulfate particles to cloud condensation nuclei. *Scientific Reports*, *8*(1), 1–14. https://doi.org/10.1038/s41598-018-21590-9

Schmale, J., & Baccarini, A. (2021). Progress in unraveling atmospheric new particle formation and growth across the Arctic. *Geophysical Research Letters*, *48*, e2021GL094198. https://doi.org/10.1029/2021GL094198

Seethala, C., Zuidema, P., Edson, J., Brunke, M., Chen, G., Li, X. Y., et al. (2021). On assessing ERA5 and MERRA2 representations of cold-air outbreaks across the Gulf Stream. *Geophysical Research Letters*, *48*, e2021GL094364. https://doi.org/10.1029/2021GL094364

Sellegri, K., Rose, C., Marinoni, A., Lupi, A., Wiedensohler, A., Andrade, M., et al. (2019). New Particle Formation: A review of ground-based observations at mountain research stations. *Atmosphere*, *10*(9), 493. https://doi.org/10.3390/atmos10090493

Siebert, H., Stratmann, F., & Wehner, B. (2004). First observations of increased ultrafine particle number concentrations near the inversion of a continental planetary boundary layer and its relation to ground-based measurements. *Geophysical Research Letters*, *31*, L09102. https://doi.org/10.1029/2003GL019086

Smith, E. T., & Sheridan, S. C. (2020). Where do cold air outbreaks occur, and how have they changed over Time? *Geophysical Research Letters*, *47*, e2020GL086983. https://doi.org/10.1029/2020GL086983

Sorooshian, A., Anderson, B., Bauer, S. E., Braun, R. A., Cairns, B., Crosbie, E., et al. (2019). Aerosol-cloud-meteorology interaction airborne field investigations: Using lessons learned from the U.S. West coast in the design of ACTIVATE off the U.S. East coast. *Bulletin of the American Meteorological Society*, *100*(8), 1511–1528. https://doi.org/10.1175/bams-d-18-0100.1

Stein, A., Draxler, R. R., Rolph, G. D., Stunder, B. J., Cohen, M., & Ngan, F. (2015). NOAA's HYSPLIT atmospheric transport and dispersion modeling system. *Bulletin of the American Meteorological Society*, *96*(12), 2059–2077. https://doi.org/10.1175/bams-d-14-00110.1

Waddicor, D., Vaughan, G., Choularton, T., Bower, K., Coe, H., Gallagher, M., et al. (2012). Aerosol observations and growth rates downwind of the anvil of a deep tropical thunderstorm. *Atmospheric Chemistry and Physics*, *12*(14), 6157–6172. https://doi.org/10.5194/acp-12-6157-2012

Wang, Y., Zheng, G., Jensen, M. P., Knopf, D. A., Laskin, A., Matthews, A. A., et al. (2021). Vertical profiles of trace gas and aerosol properties over the Eastern North Atlantic: Variations with season and synoptic condition. *Atmospheric Chemistry and Physics*, *21*(14), 11079–11098. https://doi.org/10.5194/acp-21-11079-2021

Weber, R. J., Chen, G., Davis, D. D., Mauldin, R. L., III, Tanner, D. J., Eisele, F. L., et al. (2001). Measurements of enhanced H2SO4 and 3–4 nm particles near a frontal cloud during the First Aerosol Characterization Experiment (ACE 1). *Journal of Geophysical Research*, *106*(D20), 24107–24117. https://doi.org/10.1029/2000JD000109

Weber, R. J., McMurry, P. H., Mauldin, L., Tanner, D. J., Eisele, F. L., Brechtel, F. J., et al. (1998). A study of new particle formation and growth involving biogenic and trace gas species measured during ACE 1. *Journal of Geophysical Research*, *103*(D13), 16385–16396. https://doi.org/10.1029/97JD02465

Wehner, B., Werner, F., Ditas, F., Shaw, R. A., Kulmala, M., & Siebert, H. (2015). Observations of new particle formation in enhanced UV irradiance zones near cumulus clouds. *Atmospheric Chemistry and Physics*, *15*(20), 11701–11711. https://doi.org/10.5194/acp-15-11701-2015

Williamson, C. J., Kupc, A., Axisa, D., Bilsback, K. R., Bui, T., Campuzano-Jost, P., et al. (2019). A large source of cloud condensation nuclei from new particle formation in the tropics. *Nature*, *574*(7778), 399–403. https://doi.org/10.1038/s41586-019-1638-9

Zhao, B., Shrivastava, M., Donahue, N. M., Gordon, H., Schervish, M., Shilling, J. E., et al. (2020). High concentration of ultrafine particles in the Amazon free troposphere produced by organic new particle formation. *Proceedings of the National Academy of Sciences of the United States of America*, *117*(41), 25344–25351. https://doi.org/10.1073/pnas.2006716117

Zheng, G., Wang, Y., Wood, R., Jensen, M. P., Kuang, C., McCoy, I. L., & Wang, J. (2021). New particle formation in the remote marine boundary layer. *Nature Communications*, *12*(1), 527. https://doi.org/10.1038/s41467-020-20773-1